The evolution of single and binary stars: From X-rays to gravitational waves

Marc van der Sluys

NASA Summer School, Northwestern University, Evanston, IL, USA

July 2, 2009

NORTHWESTERN UNIVERSITY

Outline

NORTHWESTERN UNIVERSITY

Hipparcos catalogue

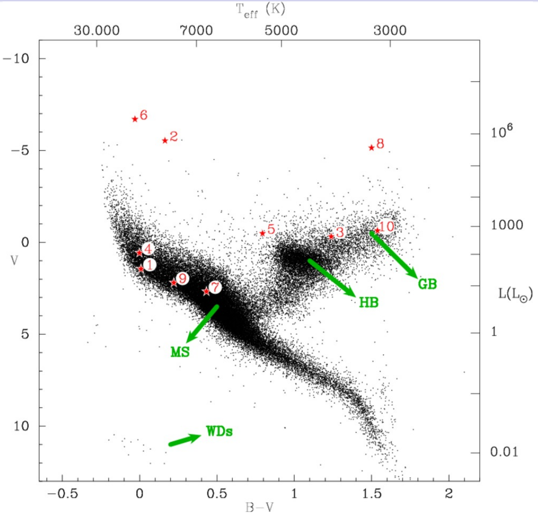

http://www.rssd.esa.int/index.php?project=HIPPARCOS

- 48 495 stars
- $\frac{\Delta d}{d} < 20\%$
- $\Delta(B-V) < 0.1$ m

1. Sirius
2. Canopus
3. Arcturus
4. Vega
5. Capella
6. Rigel
7. Procyon
8. Betelgeuse
9. Altair
10. Aldebaran

NORTHWESTERN UNIVERSITY

Main-sequence stars

Properties of single stars with solar metallicity halfway the main sequence ($X_c = 0.35$):

M ($M_\odot$)	age (Myr)	R ($R_\odot$)	L ($L_\odot$)	T_s (K)	T_c (MK)	Number density (w.r.t. 1 $M_\odot$)
0.5	52 600	0.50	0.05	3860	9.8	7.07
0.8	11 600	0.79	0.38	5100	13.4	2.34
1.0	4900	1.01	1.05	5810	15.9	1.00
1.5	1660	1.95	6.75	6660	20.9	0.131
2.0	582	2.23	20.4	8230	22.5	0.0232
2.5	405	2.80	57.8	9530	24.1	9.59×10^{-3}
3.0	246	3.09	120	10 800	25.2	3.80×10^{-3}
5.0	70.6	4.19	895	15 400	28.6	3.27×10^{-4}
10.0	12.7	5.74	8590	23 100	32.8	1.16×10^{-5}
20.0	5.18	8.78	67 900	31 300	37.0	9.3×10^{-6}
50.0	2.41	15.9	527 000	39 000	41.4	5×10^{-7}

NORTHWESTERN UNIVERSITY

Evolution of a 1 $M_\odot$ star

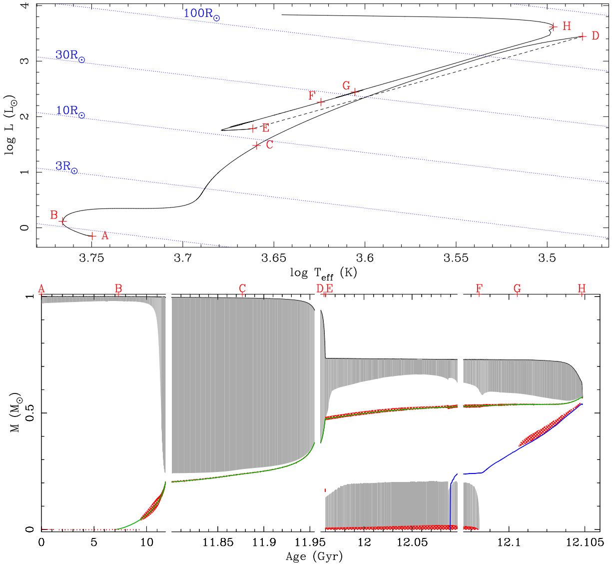

NORTHWESTERN UNIVERSITY

Evolution of a 10 $M_\odot$ star

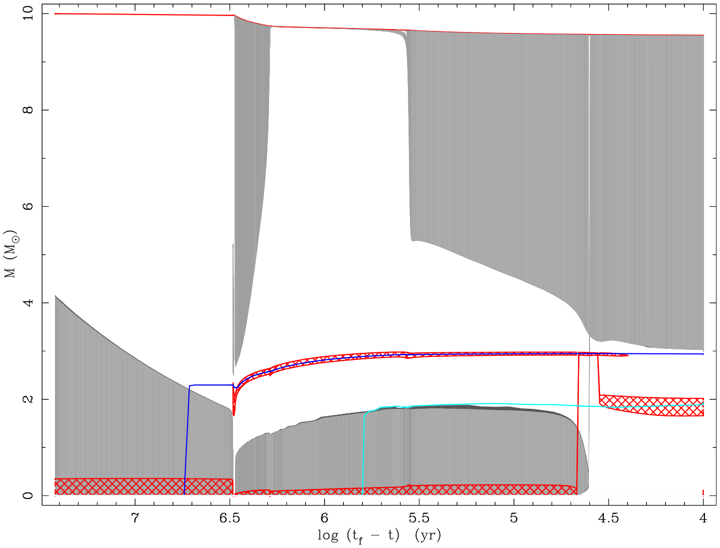

HRD for stars between 0.8 $M_\odot$ and 100 $M_\odot$

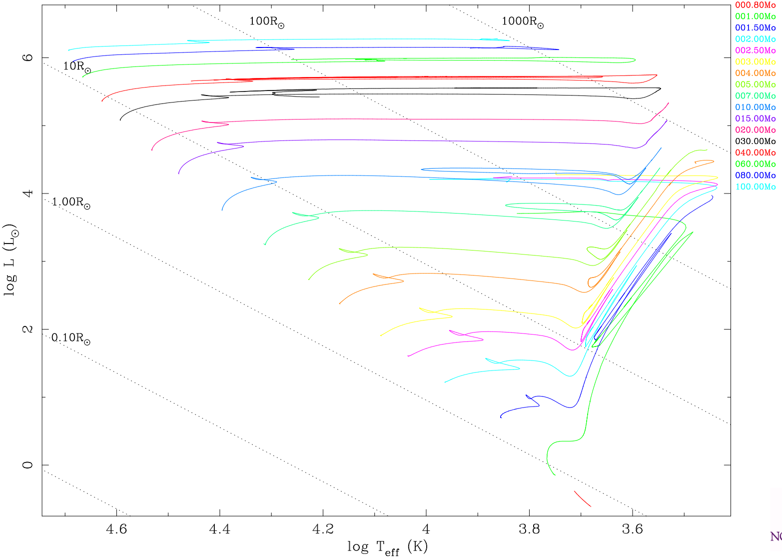

NORTHWESTERN UNIVERSITY

Onion structure for massive stars

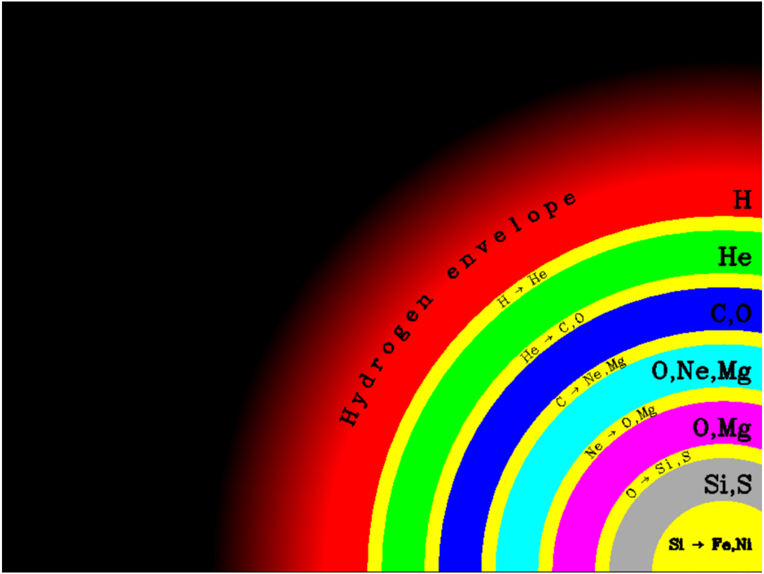

NORTHWESTERN UNIVERSITY

Burning stages of a 10 $M_\odot$ star

Stage	Net reactions	T (K)	τ
Hydrogen burning	H $\rightarrow$ He	$> 7 \times 10^6$	10 Myr
Helium burning	He $\rightarrow$ C,O	$> 2 \times 10^8$	1 Myr
Carbon burning	C $\rightarrow$ Ne,Mg	$> 8 \times 10^8$	1 kyr
Neon burning	Ne $\rightarrow$ O,Mg	$> 1.5 \times 10^9$	1 month
Oxygen burning	O $\rightarrow$ Si,S	$> 2 \times 10^9$	2 years
Silicon burning	Si $\rightarrow$ Fe,Ni	$> 3.3 \times 10^9$	3 days

Relation between ZAMS mass and remnant mass

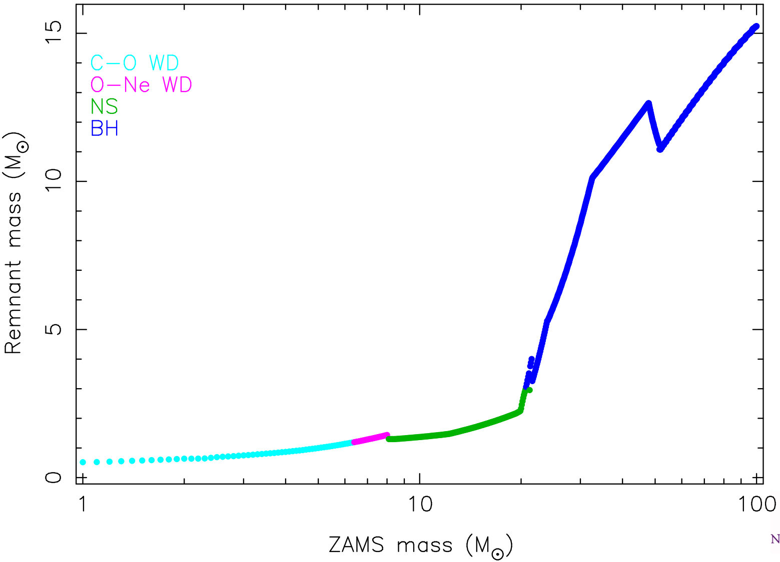

Albireo

Roche lobes

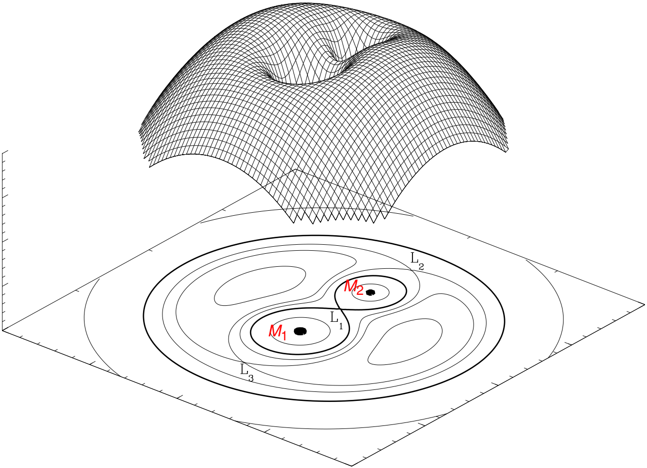

$$\frac{R_{\mathrm{Rl,i}}}{a} \approx \frac{2}{3^{4/3}} \left(\frac{M_{(3-i)}}{M_{\mathrm{T}}} \right)^{1/3}$$

accurate within 1% (?) for $q_i < 0.8$ (Paczyński, 1971).

$$\frac{R_{\mathrm{Rl,i}}}{a} \approx \frac{0.49\, q_i^{2/3}}{0.6\, q_i^{2/3} + \ln\left(1 + q_i^{1/3}\right)}$$

accurate within 1% for $0 < q_i < \infty$

(Eggleton, 1983).

NORTHWESTERN UNIVERSITY

Conservative mass transfer

Angular momentum for binary component i in a circular orbit:

$$J_i = |\vec{J}_i| = M_i \left|\vec{v}_i \times \vec{a}_i\right| = M_i v_i a_i = M_i a_i^2 \omega$$

$$J = J_1 + J_2 = \mu a^2 \omega = G^{2/3} \frac{M_1 M_2}{M_{\mathrm{T}}^{1/3}} \left(\frac{P}{2\pi}\right)^{1/3}$$

$$\frac{\dot{J}}{J} = \frac{\dot{M}_1}{M_1} + \frac{\dot{M}_2}{M_2} - \frac{1}{3}\frac{\dot{M}_{\mathrm{T}}}{M_{\mathrm{T}}} + \frac{1}{3}\frac{\dot{P}}{P}$$

Conservative: $\dot{J} = 0$, $\dot{M}_{\mathrm{T}} = 0$:

$$\frac{\dot{P}}{P} = 3\,\dot{M}_1 \frac{M_2 - M_1}{M_1 M_2}$$

NORTHWESTERN UNIVERSITY

Conservative mass transfer

Mass and angular-momentum loss

Non-conservative mass transfer (lose fraction β of transferred mass):

$$\left(\frac{\dot{J}}{J}\right)_{\rm MT} = -\alpha(1-\beta)\frac{M_i}{M_{(3-i)}}\frac{\dot{M}_i}{M_{\rm T}},$$

Gravitational waves (Peters, 1964):

$$\left(\frac{\dot{J}}{J}\right)_{\rm GW} = -\frac{32}{5}\frac{G^{5/3}}{c^5}\left(\frac{2\pi}{P}\right)^{8/3}\frac{M_1 M_2}{M_{\rm T}^{1/3}}$$

Magnetic braking, *e.g.* Verbunt & Zwaan, 1981:

$$\left(\frac{dJ}{dt}\right)_{\rm MB} = -3.8\times10^{-30} M R^4 \omega^3 \ {\rm dyn\ cm}$$

Magnetic braking, *e.g.* Sills et al., 2000:

$$\left(\frac{dJ}{dt}\right)_{\rm MB} = -K\left(\frac{R}{R_\odot}\right)^{1/2}\left(\frac{M}{M_\odot}\right)^{-1/2}\omega^3, \quad \omega \le \omega_{\rm crit}$$

$$= -K\left(\frac{R}{R_\odot}\right)^{1/2}\left(\frac{M}{M_\odot}\right)^{-1/2}\omega\omega_{\rm crit}^2, \quad \omega > \omega_{\rm crit}$$

NORTHWESTERN UNIVERSITY

Low-mass X-ray binaries

Mechanism

- Low-mass star transfers mass to neutron star or black hole
- Gravitational acceleration causes X-rays:

$$L_\mathrm{x} \approx \frac{GM_\mathrm{ns}}{R_\mathrm{ns}} \dot{M}_\mathrm{tr}$$

- Optical radiation comes from reprocessed X-rays in accretion disk

BinSim

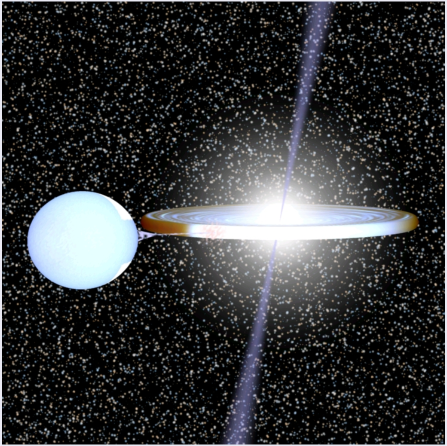

BinSim, R. Hynes, LSU

The X-ray sky

X-ray binaries

- Bright X-ray sources: in galactic plane, concentrated towards galactic centre
- 13 bright X-ray sources in globular clusters
- Binaries with $P_{\rm orb} \lesssim 60$ min are called *ultra-compact*

Ariel V X-ray map of the sky

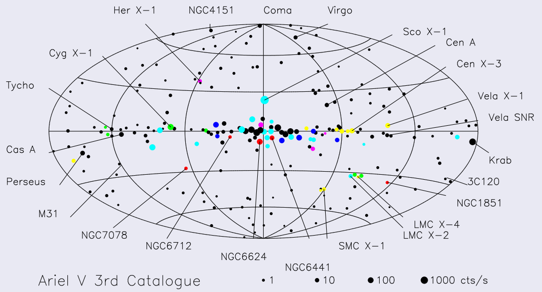

XRBs are over-abundant in GCs:

- 1 in 10^9 stars in galaxy is XRB
- 1 in 10^6 stars in globular clusters is XRB

M 15/NGC 7078 – HST

Optical counterparts

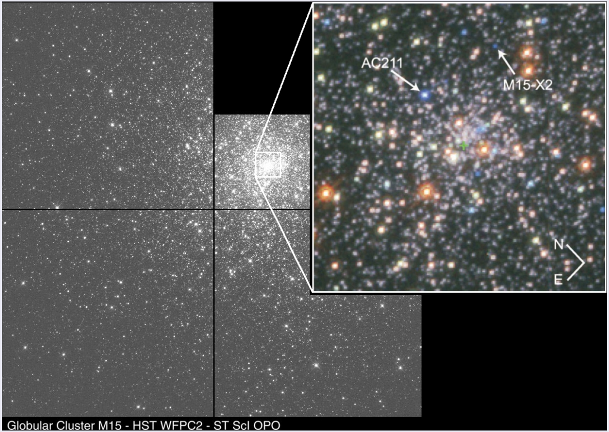

White & Angelini, 2001; Guhathakurta, 1996

NORTHWESTERN UNIVERSITY

Direct period measurement

Period for M 15-X2

Dieball et al.:

- FUV study (less crowding)
- Magnitude modulation: 0.06m
- $>$ 3000 cycles
- Period: 22.6 min.

Magnitude modulation

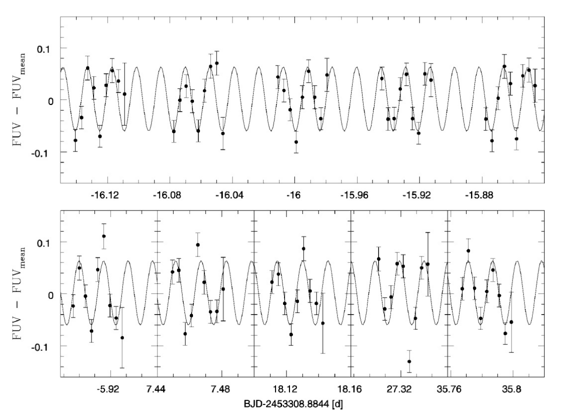

Dieball et al., 2005

Indirect period indication

Optical vs. X-ray flux

- Optical flux from reprocessed X-rays in disk
- Scales with X-ray flux and size of disk
- Hence, $f_{\rm opt}/f_{\rm X} \propto R_{\rm disk} \propto a_{\rm orb}$

Van Paradijs & McClintock, 1994

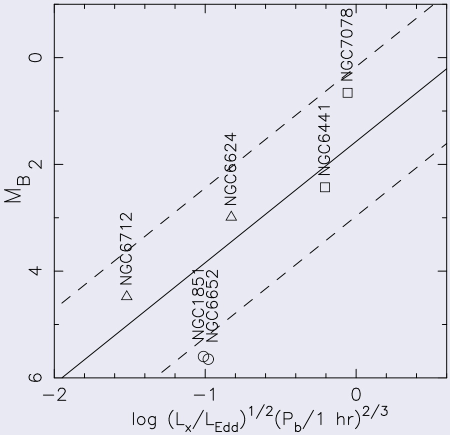

□ normal P △ ultra-short P O unknown P

Verbunt & Lewin, 2006, in "Compact Stellar X-ray Sources"

X-ray sources in globular clusters

Known period information

Cluster	Position	P_{orb}	Indirect indication		
			low f_{opt}/f_x	burst max.	X-spect.
NGC 1851	0512–40	?	U	U	U
NGC 6440	1745–20	8.7 hr	—	—	N
NGC 6441	1746–37	5.7 hr	—	N	N
NGC 6624	1820–30	11.4 min	U	U	U
NGC 6652	1836–33	?	U	U	U
NGC 6712	1850–09	21/13 min	U	U	U
NGC 7078	2127+12b	17.1 hr	—	—	—
NGC 7078	2127+12a	22.6 min	—	U	—
Terzan 1	1732–30	?	—	—	—
Terzan 2	1724–31	?	—	U	N
Terzan 5	1745–25	?	—	—	U
Terzan 6	1751–31	12.4 hr	—	—	N
Liller 1	1730–33	?	—	—	—

- Up to 6 of the 13 X-ray binaries in globular clusters are ultra-compact!
- 11-min system has negative $\dot{P}$

Scenario 1: Magnetic braking

Magnetic wind

- Rotating stars can have magnetic fields
- Evolved stars can have strong winds
- Stellar wind follows magnetic-field lines
- Star loses angular momentum efficiently
- Tidal coupling causes orbit to shrink in case of a binary

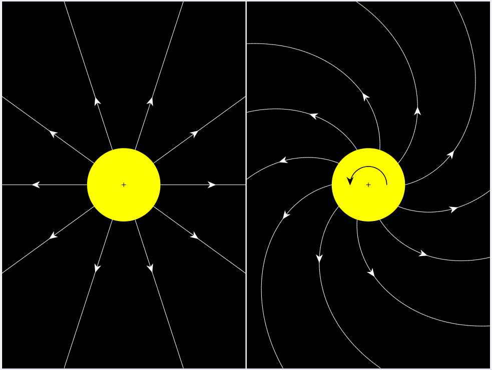

Magnetic capture

Scenario

- Low-mass donor
- Mass transfer starts after main sequence
- Lose angular momentum through MB
- Minimum period can be as low as 5 min.
- Period derivative can be negative

Example

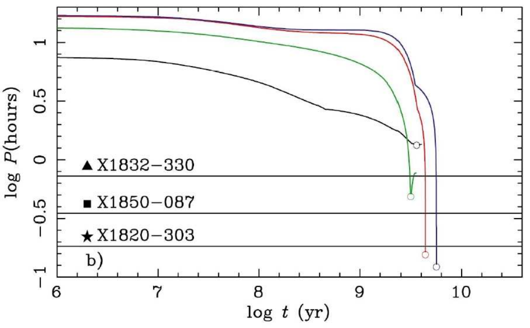

Podsiadlowski et al., 2002

Binary-evolution models

Behaviour

- Models with low P_i converge and rebound at $P_\mathrm{orb} \sim 70\,\mathrm{min}$
- Models with high P_i diverge
- Narrow range of P_i leads to ultra-short period

Example for $Z = 0.01$, $1.1\,M_\odot$

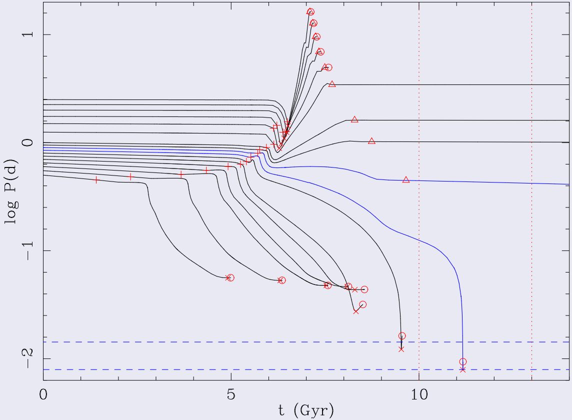

+ MT starts × P_min △ MT ends O model ends

Van der Sluys, Verbunt & Pols, 2005a

Creating a population

Find the orbital period P at a random moment in time for a random P_{i}

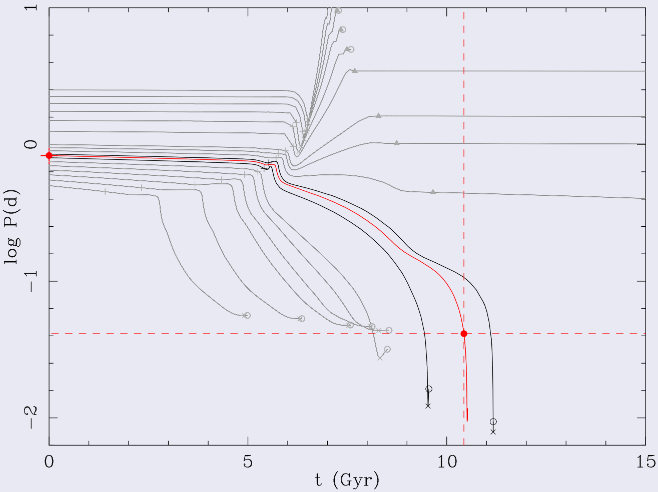

Statistics

Results for a given donor mass

- Generate 10^6 systems
- Some artefacts at long periods
- Short-period distribution is representative

$Z = 0.01$, $1.1\ M_\odot$, 10^6 binaries

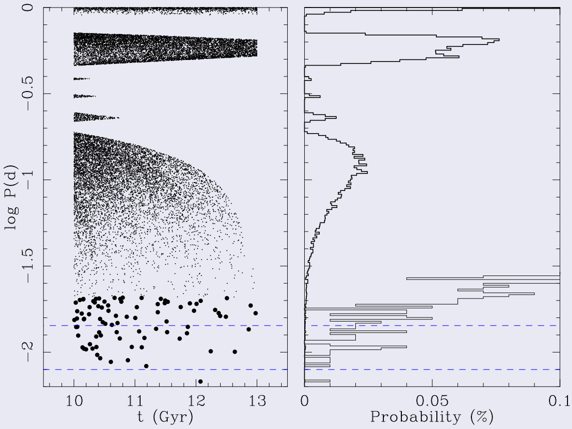

Van der Sluys, Verbunt & Pols, 2005a

Statistics: compare magnetic-braking prescriptions

Different MB ‘law’

- Use more realistic, saturated MB
- Lower limit for saturated MB similar to that for no MB
- No systems below $\sim$ 70 min

$Z = 0.01$, 10^7 binaries

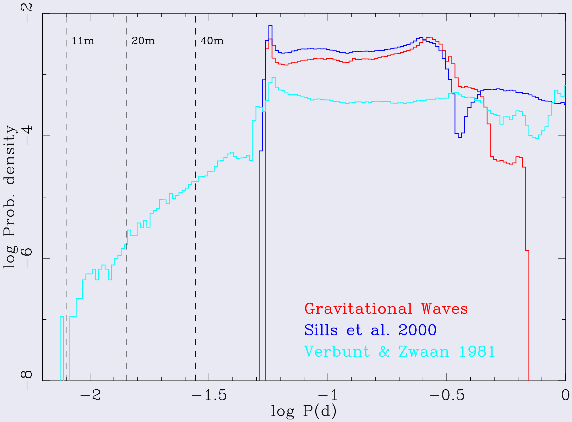

Van der Sluys, Verbunt & Pols, 2005b

Conclusions

Magnetic capture

- Magnetic capture produces too few ultra-compact X-ray binaries
- More realistic, weaker magnetic-braking laws predict no UCXBs at all
- Magnetic capture cannot explain the observations

Stellar collisions

- (Sub)giant collides with neutron star and forms NS-WD binary
- Gravitational waves cause orbital shrinkage until mass transfer starts
- $\dot{P}$ must be positive
- Measured negative $\dot{P}$ should then be explained by acceleration

Observed double white dwarfs

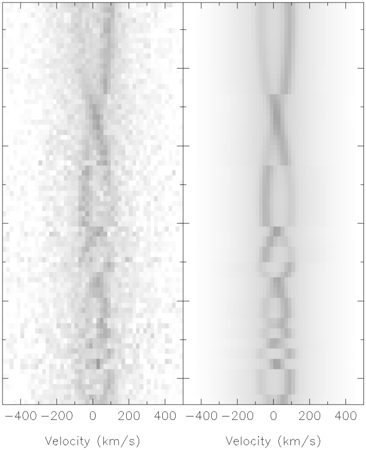

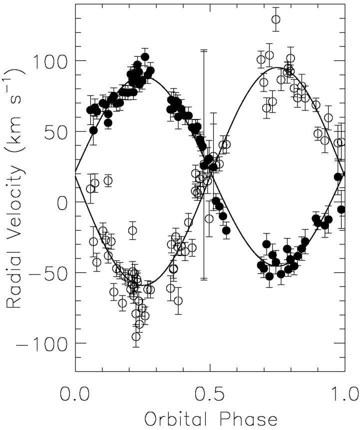

WD 0316+768, Adapted from Maxted et al., 2002

NORTHWESTERN UNIVERSITY

Observed double white dwarfs

System	*Porb* (d)	*aorb* ($R_\odot$)	M_1 ($M_\odot$)	M_2 ($M_\odot$)	q_2 (M_2/M_1)	$\Delta\tau$ (Myr)
WD 0135–052	1.556	5.63	0.52 ± 0.05	0.47 ± 0.05	0.90 ± 0.04	350
WD 0136+768	1.407	4.99	0.37	0.47	1.26 ± 0.03	450
WD 0957–666	0.061	0.58	0.32	0.37	1.13 ± 0.02	325
WD 1101+364	0.145	0.99	0.33	0.29	0.87 ± 0.03	215
PG 1115+116	30.09	46.9	0.7	0.7	0.84 ± 0.21	160
WD 1204+450	1.603	5.74	0.52	0.46	0.87 ± 0.03	80
WD 1349+144	2.209	6.59	0.44	0.44	1.26 ± 0.05	—
HE 1414–0848	0.518	2.93	0.55 ± 0.03	0.71 ± 0.03	1.28 ± 0.03	200
WD 1704+481a	0.145	1.14	0.56 ± 0.07	0.39 ± 0.05	0.70 ± 0.03	-20[a]
HE 2209–1444	0.277	1.88	0.58 ± 0.08	0.58 ± 0.03	1.00 ± 0.12	500

[a] Unclear which white dwarf is older

See references in: Maxted et al., 2002 and Nelemans & Tout, 2005.

NORTHWESTERN UNIVERSITY

Common envelope

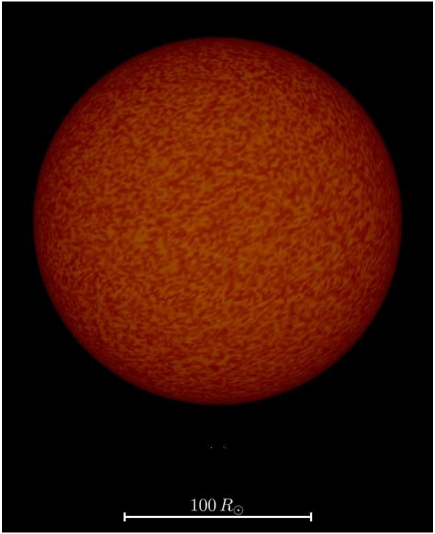

- Average orbital separation:
  - $7\ R_\odot$
- Typical progenitor:
  - $M_c \gtrsim 0.3\,M_\odot$
  - $R_* \sim 100\,R_\odot$

NORTHWESTERN UNIVERSITY

Common envelope

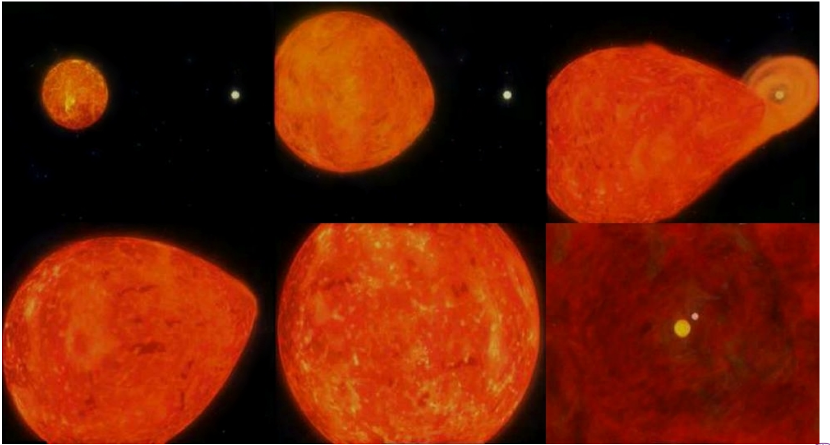

Envelope ejection

- Classical α-common envelope (spiral-in):
  - orbital energy is used to expel envelope (Webbink, 1984):

$$U_{\rm bind} = \alpha_{\rm CE} \left[\frac{G\, M_{1\rm f}\, M_2}{2\, a_{\rm f}} - \frac{G\, M_{1\rm i}\, M_2}{2\, a_{\rm i}} \right]$$

  - $\alpha_{\rm CE}$ is the common-envelope efficiency parameter

- γ-envelope ejection (EE, spiral-in not necessary):
  - envelope ejection with angular-momentum balance (Nelemans et al., 2000):

$$\frac{J_{\rm i} - J_{\rm f}}{J_{\rm i}} = \gamma_{\rm CE} \frac{M_{1\rm i} - M_{1\rm f}}{M_{1\rm i} + M_2}$$

  - $\gamma_{\rm CE} \approx 1.5$ is the efficiency parameter

NORTHWESTERN UNIVERSITY

Envelope ejection

Assumption:

- Envelope ejection occurs much faster than nuclear evolution, hence:
  - core mass does not grow during envelope ejection
  - no accretion by companion during envelope ejection

From Eggleton models:

- White-dwarf mass fixes evolutionary state of progenitor
- Giant radius determines orbital period of progenitor
- Envelope binding energy dictates what α_{CE} is needed

Progenitor models

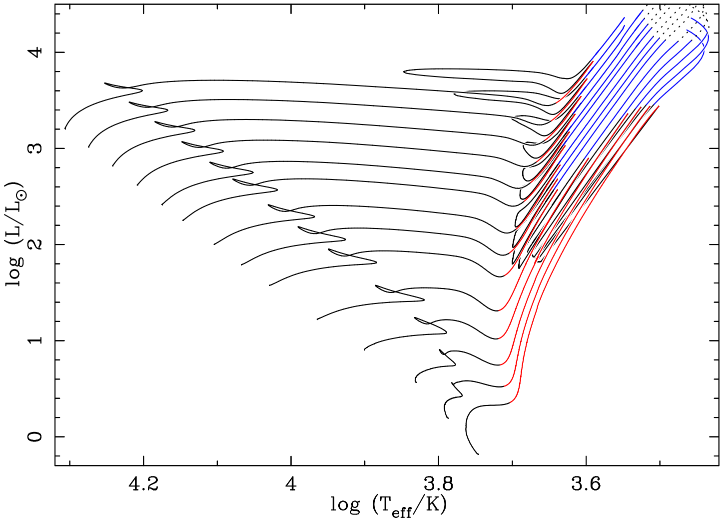

Eggleton code

199 singe-star models

0.8-10 $M_\odot$

RGB

AGB

Progenitor models

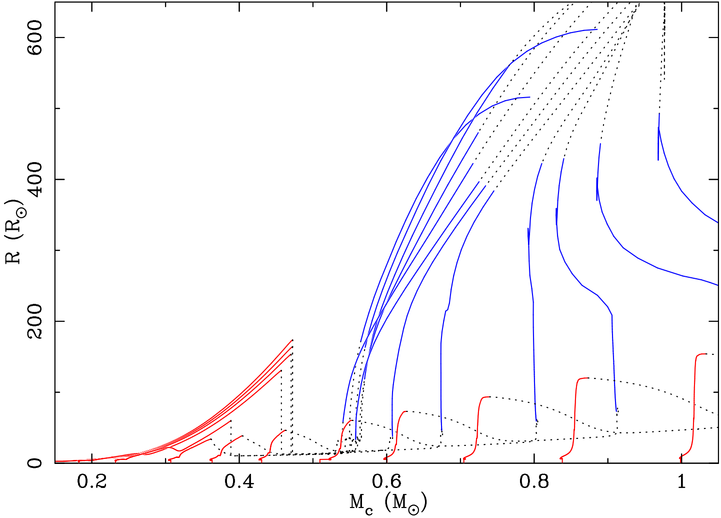

R_* provides P_{orb} at onset of EE

RGB

AGB

Progenitor models

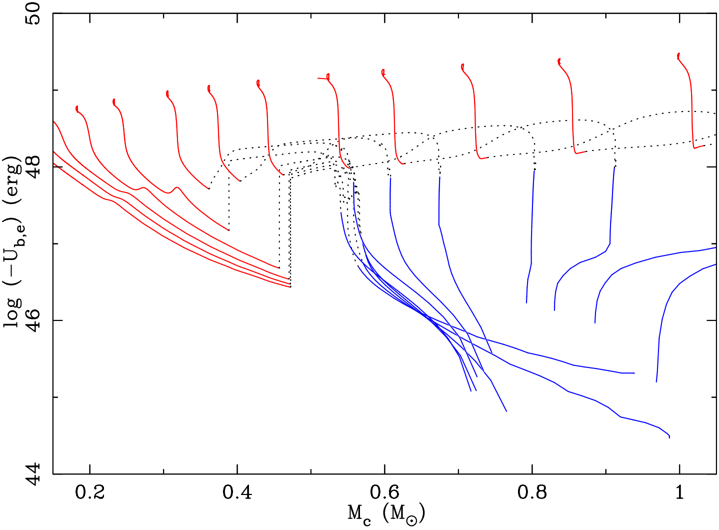

Envelope U_{bind} provides α_{CE}

RGB

AGB

Evolutionary scenarios

Stable + unstable

MS + MS

↓ Stable M.T. (cons.) ↓

WD + MS

↓ Unstable M.T. (α-CE) ↓

WD + WD

Unstable + unstable

MS + MS

↓ Unstable M.T. (γ-EE) ↓

WD + MS

↓ Unstable M.T. (α, γ-EE) ↓

WD + WD

Conservative first mass transfer

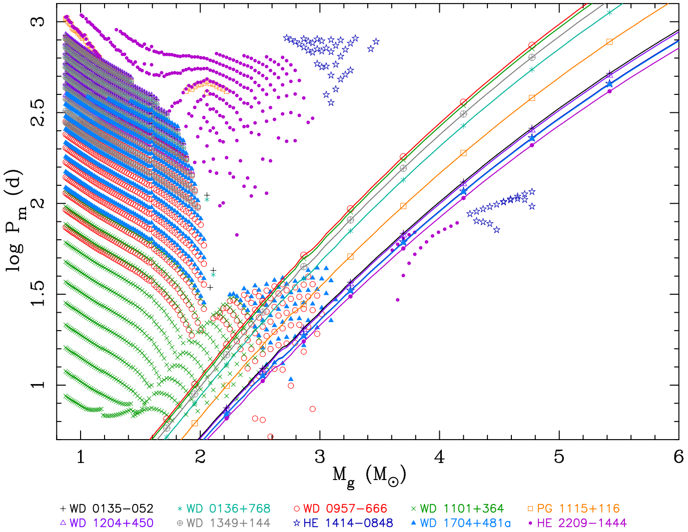

Maximum P_{orb} after stable mass transfer with $q_i = 0.62$

(Nelemans et al., 2000)

Only 5 systems have CE solutions with $P_{orb} < P_{max}$

Conservative first mass transfer

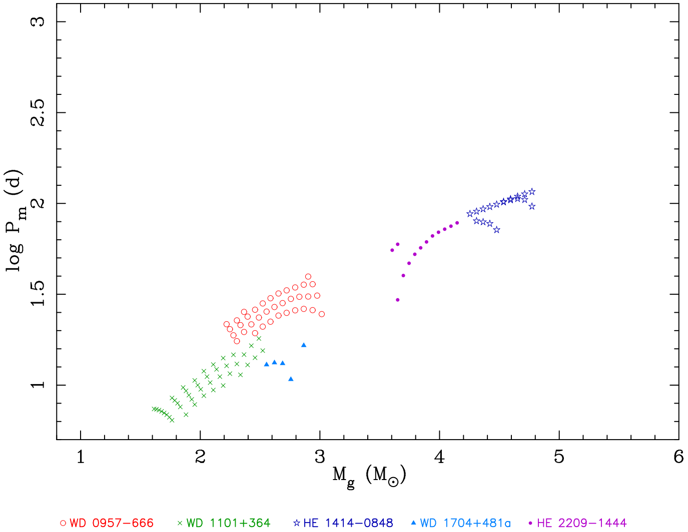

CE solutions that may be formed by stable mass transfer

Conservative mass transfer: M_{tot} and J_{orb} fixed

One free parameter: q_i

NORTHWESTERN UNIVERSITY

Conservative mass transfer: q, Δt

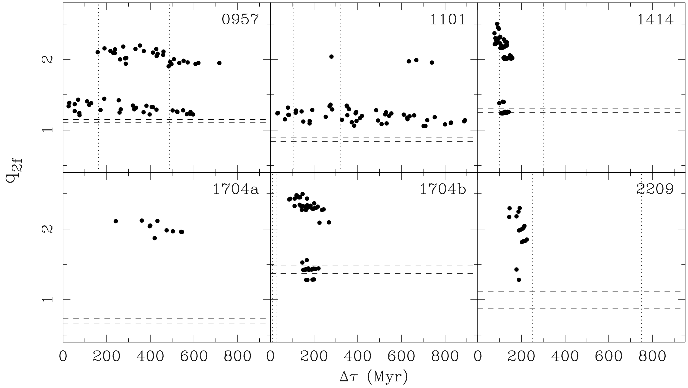

1414 fits

0957, 1101, 1704b and **2209** nearly fit

Out of ten systems, 1 can be explained, 4 are close

Angular-momentum balance

- Average specific angular momentum of the system:

$$\frac{J_\mathrm{i} - J_\mathrm{f}}{J_\mathrm{i}} = \gamma_\mathrm{s} \frac{M_{1\mathrm{i}} - M_{1\mathrm{f}}}{M_{\mathrm{tot,i}}}$$

- Specific angular momentum of the accretor:

$$\frac{J_\mathrm{i} - J_\mathrm{f}}{J_\mathrm{i}} = \gamma_\mathrm{a} \left[1 - \frac{M_{\mathrm{tot,i}}}{M_{\mathrm{tot,f}}} \exp\left(\frac{M_{1\mathrm{f}} - M_{1\mathrm{i}}}{M_2}\right)\right]$$

- Specific angular momentum of the donor:

$$\frac{J_\mathrm{i} - J_\mathrm{f}}{J_\mathrm{i}} = \gamma_\mathrm{d} \frac{M_{1\mathrm{i}} - M_{1\mathrm{f}}}{M_{\mathrm{tot,f}}} \frac{M_{2\mathrm{i}}}{M_{1\mathrm{i}}}$$

Models

- Number of progenitor models:
  - 10+1 observed systems
  - 199 progenitor models in our grid
  - 11 variations in observed mass: $-0.05, -0.04, ..., +0.05\ M_\odot$
  - total: $11 \times 11 \times \sum_{n=1}^{198} n \approx$ **2.4 million**
- Filters:
  - dynamical MT: $R_* > R_\mathrm{BGB}$ and $q > q_\mathrm{crit}$
  - age: $\tau_1 < \tau_2 < 13\,\mathrm{Gyr}$
  - EE-parameter: $0.1 < \alpha_\mathrm{ce}, \gamma < 10$
- Candidate progenitors left: $\sim$ **204 000**

Results for $\gamma_d + \gamma_a$

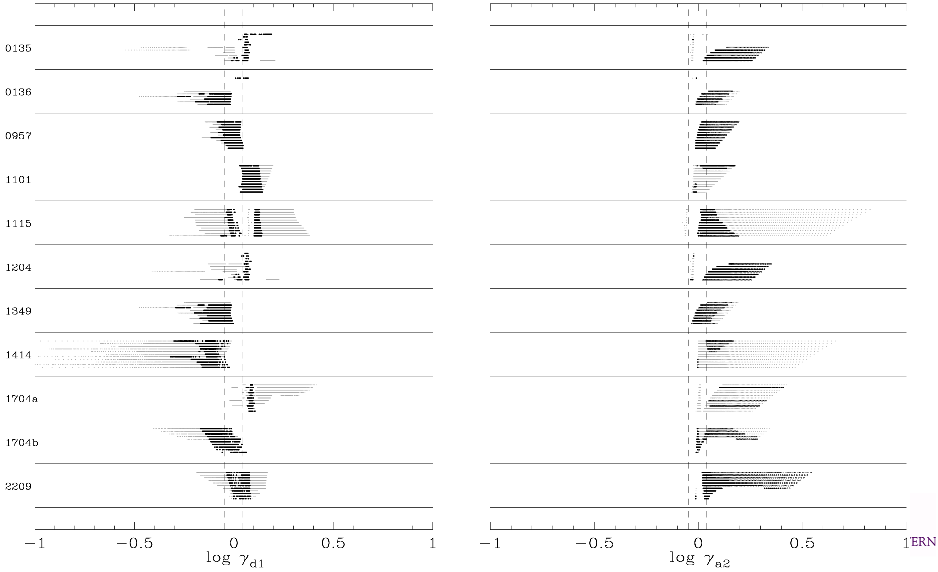

Results: overview

Select systems with:

- $0.8 < \alpha_{ce} < 1.2$
- $1.46 < \gamma_s < 1.79$
- $0.9 < \gamma_{a,d} < 1.1$

System	1: $\gamma_s\alpha_{ce}$	2: $\gamma_s\gamma_s$	3: $\gamma_a\alpha_{ce}$	4: $\gamma_a\gamma_a$	5: $\gamma_d\alpha_{ce}$	6: $\gamma_d\gamma_a$	Best:
0135	$-/-$	$+/\sim$	$+/\sim$	$-/-$	$+/\sim$	$+/\sim$	2,3,5,6
0136	$+/+$	$+/+$	$+/\sim$	$+/\sim$	$+/+$	$+/+$	1,2,5,6
0957	$+/+$	$+/+$	$-/-$	$+/-$	$+/+$	$+/+$	1,2,5,6
1101	$+/\sim$	$+/-$	$+/-$	$-/-$	$+/\sim$	$+/\sim$	1,5,6
1115	$+/\sim$	$+/+$	$+/\sim$	$+/\sim$	$+/+$	$+/+$	2,5,6
1204	$-/-$	$+/-$	$+/-$	$+/-$	$+/-$	$+/+$	6
1349	$+/+$	$+/+$	$+/+$	$+/+$	$+/+$	$+/+$	1–6
1414	$-/-$	$+/+$	$-/-$	$+/+$	$-/-$	$+/+$	2,4,6
1704a	$+/-$	$+/-$	$-/-$	$-/-$	$-/-$	$-/-$	1,2
1704b	$+/-$	$+/-$	$-/-$	$+/-$	$+/-$	$+/-$	1,2,4,5,6
2209	$+/+$	$+/+$	$-/-$	$-/-$	$+/\sim$	$+/+$	1,2,6

$+$: α, γ within range, $-$: α, γ outside range

$+$: $\Delta(\Delta t) < 50\%$, $\sim$: $50\% < \Delta(\Delta t) < 500\%$, $-$: $\Delta(\Delta t) > 500\%$

NORTHWESTERN UNIVERSITY

Results: example solution

WD 0136+768

	Age (Gyr)	$M_1(M_\odot)$	$M_2(M_\odot)$	P_{orb}(d)
	0.000	1.70	1.59	106.10
$\gamma_d = 0.96 \rightarrow$	1.940	1.70	1.59	106.10
	1.940	0.37	1.59	371.40
$\gamma_a = 1.05 \rightarrow$	2.390	0.37	1.59	371.40
$\Delta\tau = 450$ Myr $\rightarrow$	2.540	0.37	0.46	1.41

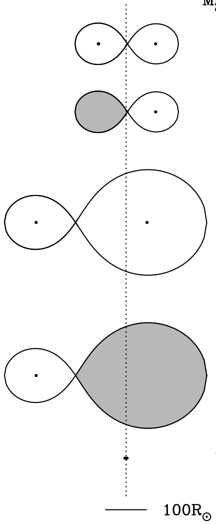

Results: solutions

WD	Mthd.	γ_1	γ_2, α_{ce2}	$\Delta\tau$/Myr obs	mdl	M_{1i} $M_\odot$	M_{2i} $M_\odot$	P_i d	P_m d	M_{1f} $M_\odot$	M_{2f} $M_\odot$	P_f d
0135	$\gamma_d\gamma_a$	1.11	0.94	350	118	3.30	2.90	36.28	41.10	0.47	0.42	1.56
0136	$\gamma_d\gamma_a$	0.96	1.05	450	450	1.70	1.59	106.1	371.4	0.37	0.46	1.41
0957	$\gamma_d\gamma_a$	1.00	1.01	325	317	1.98	1.83	26.17	79.26	0.33	0.37	0.06
1101	$\gamma_d\gamma_a$	1.10	0.98	215	322	2.87	2.34	22.02	28.23	0.39	0.34	0.14
1115	$\gamma_d\gamma_a$	0.97	1.04	160	240	5.42	3.42	201.2	1012.	0.89	0.75	30.09
1204	$\gamma_d\gamma_a$	1.09	0.92	80	100	3.34	2.98	15.47	19.99	0.47	0.41	1.60
1349	$\gamma_d\gamma_a$	0.95	0.98	0	101	1.86	1.81	63.44	241.2	0.35	0.44	2.21
1414	$\gamma_d\gamma_a$	0.95	0.99	200	188	3.51	3.09	70.81	358.3	0.52	0.66	0.52
1704a	$\gamma_d\gamma_a$	1.11	1.13	-20	52	2.06	1.88	40.37	65.66	0.51	0.36	0.14
1704b	$\gamma_d\alpha_{ce}$	1.03	0.15	20	182	1.68	1.65	212.1	478.6	0.41	0.58	0.14
2209	$\gamma_d\gamma_a$	1.04	1.05	500	340	4.15	2.94	98.45	294.3	0.63	0.63	0.28

Conclusions double white dwarfs

- Conservative mass transfer cannot explain the observed double white dwarfs
- Unstable envelope ejection can do this
- Several EE descriptions can reconstruct observed masses and periods
- $\gamma_s\gamma_s$ and $\gamma_d\gamma_a$ can in addition explain most observed cooling-age differences

NORTHWESTERN UNIVERSITY

Laser Interferometer GW Observatory

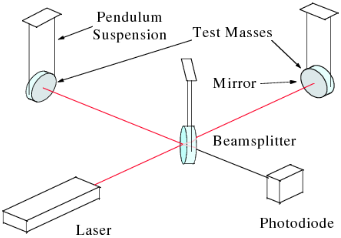

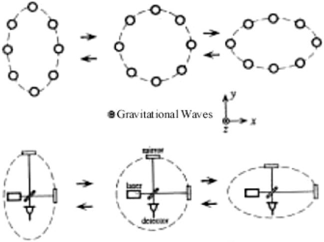

NORTHWESTERN UNIVERSITY

Goals of this project

LIGO

- Show that Markov-Chain Monte Carlo (MCMC) with a large number of parameters (12–15) on LIGO data can be done
- Automated parameter estimation on detected inspiral signal:
  - Confirm spinning inspiral nature of signal
  - Determine physical parameters (masses, spin, position, . . .)

Astrophysics

- BH/NS mass distributions, BH spins and spin alignments
- Association of GW and EM events, *e.g.* GRB
- Merger rates, NS-NS/BH-NS/BH-BH merger ratios
- Evolution of massive stars (in binaries), CEs
- Initial-mass range for BH progenitors

Predicted detection rates

Realistic estimate:

	Rates (yr^{-1})			Horizon (Mpc)		
	NS-NS	BH-NS	BH-BH	NS-NS	BH-NS	BH-BH
Initial	0.015	0.004	0.01	32	67	160
Enhanced	0.15	0.04	0.11	71	149	349
Advanced	20	5.7	16	364	767	1850

Plausible, optimistic estimate:

	Rates (yr^{-1})			Horizon (Mpc)		
	NS-NS	BH-NS	BH-BH	NS-NS	BH-NS	BH-BH
Initial	0.15	0.13	1.7	32	67	160
Enhanced	1.5	1.4	18	71	149	349
Advanced	200	190	2700	364	767	1850

Estimates assume $M_{\rm NS} = 1.4\,M_\odot$ and $M_{\rm BH} = 10\,M_\odot$

CBC group, rates document

Inspiral waveforms

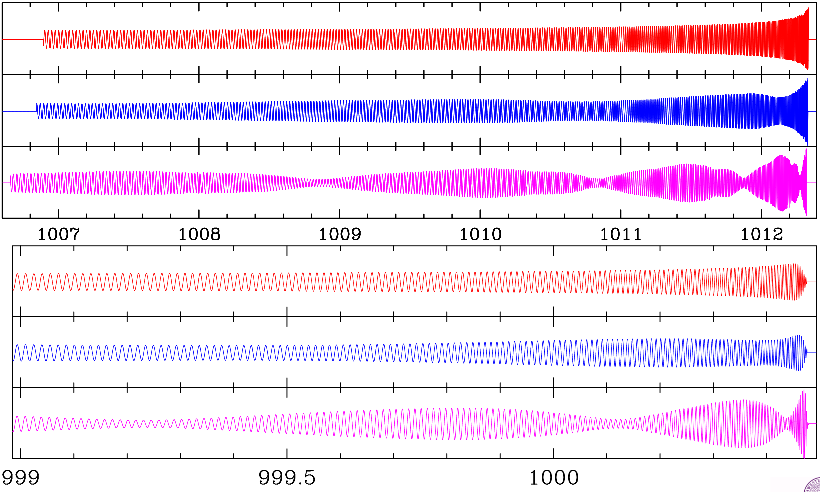

$a_{\text{spin}} \equiv S/M^2 =$ 0.0, 0.1 and 0.5

Signal injection into detector noise

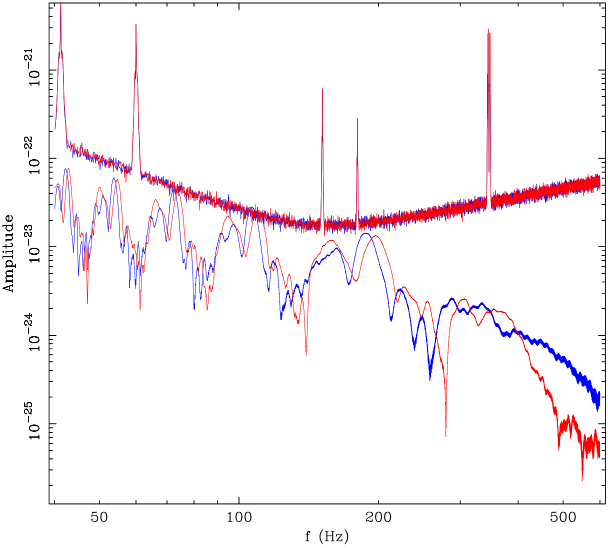

- Using 1–2 4-km detectors H1, L1
- Gaussian, stationary noise
- Do 1.5PN software injections
- Retrieve physical parameters with 1.5PN template

Here, ΣSNR = 17

NORTHWESTERN UNIVERSITY

Compute posterior distribution

- Find posterior density of the model parameters
- Bayesian approach
- The likelihood for each detector i is:

$$L_i(d|\vec{\lambda}) \propto \exp\left(-2\int_0^\infty \frac{\left|\tilde{d}(f) - \tilde{m}(\vec{\lambda}, f)\right|^2}{S_n(f)}\, df\right) \propto \exp\left(\frac{\mathrm{SNR}^2}{2}\right)$$

- Coherent network of detectors:
  - $\mathrm{PDF}(\vec{\lambda}) \propto \mathrm{prior}(\vec{\lambda}) \times \prod_i L_i(d|\vec{\lambda})$
- Use Markov-Chain Monte Carlo to sample the posterior

Markov chains

- Choose starting point for chain: $\vec{\lambda}_1$
- Calculate its likelihood: $L_j \equiv L(d|\vec{\lambda}_j)$
- do $j = 1, N$
  - draw random jump size $\Delta\vec{\lambda}_j$ from Gaussian with $\vec{\sigma}$
  - consider new state $\vec{\lambda}_{j+1} = \vec{\lambda}_j + \Delta\vec{\lambda}_j$
  - calculate $L_{j+1} \equiv L(d|\vec{\lambda}_{j+1})$
  - if($\frac{L_{j+1}}{L_j} >$ ran_unif[0,1]) then
    - Accept new state $\vec{\lambda}_{j+1}$
    - Increase jump size $\vec{\sigma}$
  - else
    - Reject new state; $\vec{\lambda}_{j+1} = \vec{\lambda}_j$
    - Decrease jump size $\vec{\sigma}$
  - end if
  - save state $\vec{\lambda}_{j+1}$
- end do (j)

NORTHWESTERN UNIVERSITY

MCMC example

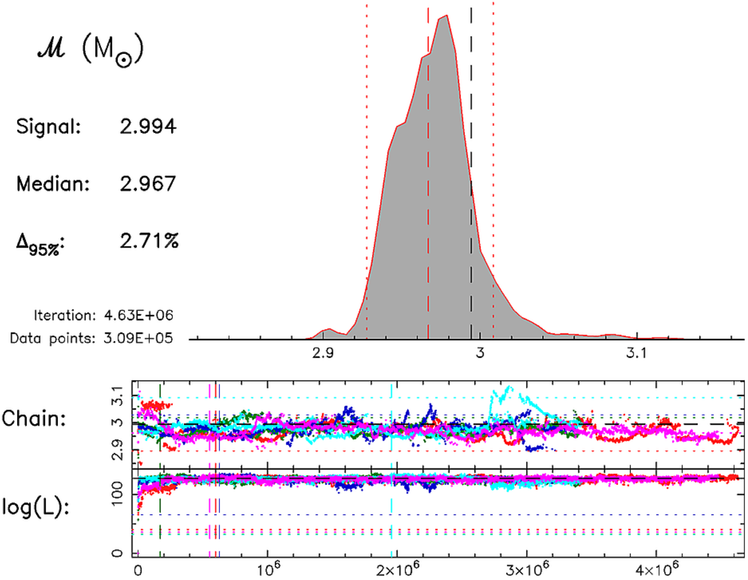

MCMC runs

MCMC parameters

masses: M_c & η, distance: $\log d_L$, time and phase at coalescence: t_c & φ_c, position: R.A. & sin Dec, spin magnitude: $a_{spin_{1,2}}$, spin orientation: $\cos\theta_{spin_{1,2}}$ & $\varphi_{spin_{1,2}}$, orientation: $\cos(\iota)$ & ψ

MCMC set-up

- 5 serial chains per run, starting from the true parameter values
- Chain length: 5×10^6 states, burn-in: 5×10^5 states
- Run time: 10 days on a 2.8 GHz CPU

- Signals injected in simulated noise for H1L1 @ SNR $\approx$17.0
- Fiducial binary: $M_{1,2} = 10 + 1.4\, M_\odot$, d_L = 16–21 Mpc
- Spin: $a_{spin} = 0.0, 0.1, 0.5, 0.8$, $\theta_{SL} = 20°, 55°$

Spinning MCMC results

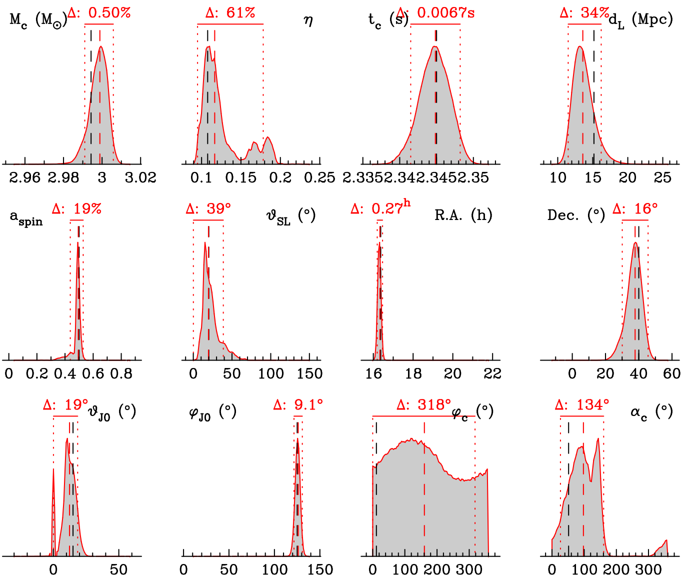

Parameters:

- H1 & L1
- $M = 10, 1.4\,M_\odot$
- $d_L = 18.7\,\mathrm{Mpc}$
- $a_{\mathrm{spin}} = 0.5$, $\theta_{\mathrm{SL}} = 20°$
- ΣSNR ≈ 17.0
- Black dashed line: true value
- Red dashed line: median
- Δ's: 90% probability

NORTHWESTERN UNIVERSITY

Spinning MCMC results

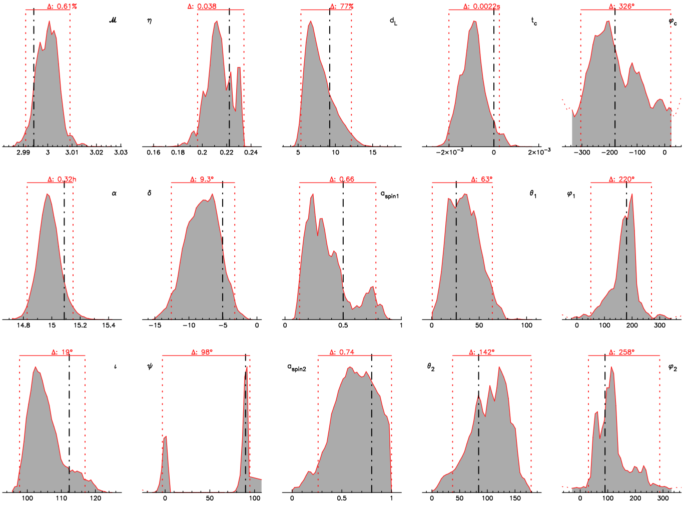

- 3.5-pN waveform
- 3 detectors
- $\mathcal{M} = 3.0$, $\eta = 0.22$
- $a_{\rm spin} = 0.5, 0.8$
- Σ SNR=20

NORTHWESTERN UNIVERSITY

Spinning MCMC results

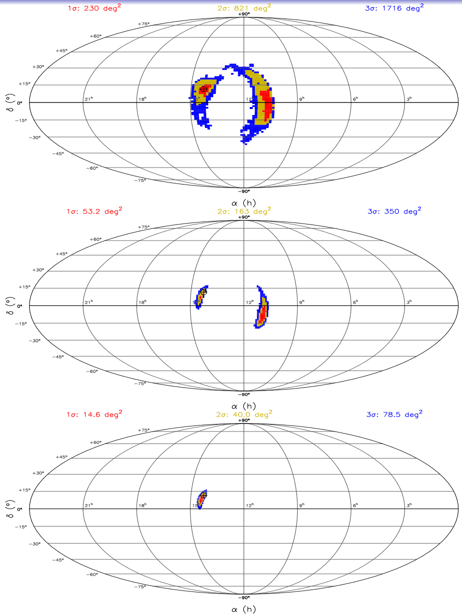

Spinning BH, non-spinning NS:

$10 + 1.4\,M_\odot$, 16–22 Mpc,

Σ SNR=17

2 detectors, $a_{\rm spin} = 0.0$

2 detectors, $a_{\rm spin} = 0.5$

3 detectors, $a_{\rm spin} = 0.5$

van der Sluys et al., 2008; Raymond et al., 2009

Conclusions GW parameter estimation

MCMC code:

We have developed an MCMC code that can recover the 12–15 parameters of a binary inspiral, including one or two spins

Accuracies:

- Detection with only 2 detectors can produce astronomically relevant information when spin is present, with typical accuracies for low/higher spin:
  - individual masses: $\sim 32\%/39\%$
  - dimensionless spin: $0.17 - 0.18$
  - distance: $\sim 55\%/45\%$
  - sky position: $\sim 25^\circ/7^\circ$
  - binary orientation: $\sim 55^\circ/15^\circ$
  - time of coalescence: 11ms / 6ms
- Combination of the above can lead to association with an electromagnetic detection (*e.g.* gamma-ray burst)